

STUDY ON THE CONFIGURATIONS OF DEBRIS-FLOW FANS

Y.F. TSAI^(*), H.K. TSAI^(**) & Y.L. CHENG^(***)

^(*) Professor, Department of Social and Regional Development, National Taipei University of Education, Taipei, Taiwan No.134, Sec. 2, Heping E. Rd., Da-an District, Taipei City 106, Taiwan, tyf@tea.ntue.edu.tw, +886-2-2732-1104 ext. 2236

^(**) Assistant Research Fellow, Institute of Information Science, Academia Sinica, Taipei, Taiwan

28 Academia Road, Section 2, Nankang, Taipei 115, Taiwan, hktsai@iis.sinica.edu.tw, +886-2-27883799 ext. 1718

^(***) Research assistant, Department of Social and Regional Development, National Taipei University of Education, Taipei, Taiwan No.134, Sec. 2, Heping E. Rd., Da-an District, Taipei City 106, Taiwan, superdaiwa@gmail.com, +886-2-2732-1104 ext. 2314

ABSTRACT

Studies on debris-flow fan configurations are fundamental to map hazard zone of debris flow disasters. This study aims to identify the morphological similarity of debris-flow fans based on a series of laboratory experiments and field investigations. The maximum length L_c , width B_m and thickness Z_o of debris-flow fans are adopted as the characteristic parameters for analyzing the morphological similarity. The analysis demonstrates that the non-dimensional longitudinal and transverse profiles of debris-flow fans are described by Gaussian curves, while the non-dimensional plan form is closely fitted using a circular curve. By combining the three non-dimensional curves, the three-dimensional topography of debris-flow fans are easily obtained based on the parameters L_c , B_m and Z_o . The volume V are simply related to these maximum values via $V = \alpha L_c B_m Z_o$ with an empirically determined shape parameter α . From the result of verification with a debris flow fan in Foncho Village, Nan-tou County of central Taiwan, it shows that the 3D topography function makes a good hazard zone mapping of debris flow. Furthermore, the parameter α is approximately 0.28 for a natural stony debris-flow fan.

KEY WORDS: debris flow, debris-flow fan, morphological similarity

INTRODUCTION

Debris flows are highly hazardous hydrological processes common in Taiwan. They are generally de-

scribed as gravity flows of a mixture of soil, rocks, water, and/or air. As a landslide-initiated debris flow proceeds down a steep mountain canyon, it scours materials from the channel and grows in mass. When the debris flow reaches a gentle basin from the steep channel, it spreads out, reduces its momentum and then stops after reaching a flatter area. Sediment deposits, leaves mud fluid, or clear water flowing downstream. This process gradually creates a debris-flow fan. The fan of debris-flow usually becomes a hazard zone and makes a serious damage and property loss. Therefore, the study on the hazard zone mapping of debris-flow become very important.

The process of formation and the shape of debris-flow fans have received attention by investigators such as HOOKE (1967), OKUDA (1973), OKUDA *et alii* (1977), TAKAHASHI & YOSHIDA (1979), TAKAHASHI (1980), and ASHIDA *et alii* (1980). These investigations provided information on local debris-flow fans, but did not consider the morphological similarity. Numerous researchers tried to identify the hazard zone of debris flow based on the maximum deposition length of debris-flow fan. TAKAHASHI (1991) combine the law of conservation of mass with momentum balance equation to derive the deposition length of debris flow fan. OKUDA (1973) utilized the particle dynamics method to estimate the length of debris-flow fan. CANNON (1993), OKUDA (1984), IKEYA (1981) and BATHURST *et alii* (1997) make use of statistical analysis based on historical data of field investigation to predict the spread length of debris flow. Although these previous

studies can approximately map the hazard zone they did not consider the three dimensional (3D) topography of the debris-flow fans.

Many researchers, such as SHIEH *et alii* (1996), RICKENMANN & KOCH (1997), FRACCAROLLO & PAPA (2000), LAIGLE *et alii* (2003), CETINA & KRZYK (2003), and ITOH *et alii* (2003) developed numerical models of debris-flow depositions on fans and made good simulations. While these numerical models can offer more precise simulations of debris-flow fans, but complex calculation conditions are required and these models sometimes need to adjust the models' parameters case by case.

This study aims to identify the hazard zone of debris flow via a series of investigation on the debris-flow fan configurations. We find that a simple relation exists between the volume of a debris-flow fan and its maximum length, width, and thickness from a series of experiments. The 3D topography of a debris-flow fan is also derived from this study. By utilizing the 3D topography of a debris-flow fan, we can easily map the hazard zone of debris flow. For the purpose of verification, a debris-flow fan in Foncho Village, Nantou County was investigated. The results reveal that the morphological deposition method can map the approximate hazard zone of debris flow.

LABORATORY EXPERIMENTS

EXPERIMENTAL SETUP AND CONDITIONS

A series of experiments was performed in laboratory to observe the formation process of a debris-flow fan at a steep channel mouth. The experimental facility includes a main flume and a flood basin. Fig. 1 schematically shows the experimental set-up. The main flume is 8.0-m long, 0.2-m wide, and 0.5-m deep. The flood basin with transparent sidewalls is closely connected with the downstream end of the main flume and is 3.0-m long, 2.2-m wide, and 0.5-m deep. The main flume can be tilted from 0 to 30°, and the flood basin can be tilted from 0 to 20°.

Seventy-two tests were conducted with varying gradients of the main flume and flood basin, sediment size and size distribution, supplied water, mud-fluid and sediment discharges. Table 1 summarizes the conditions of each experiment. In Table 1, d_{50} =mean diameter of the used sediment materials; C_u =uniformity coefficient defined as d_{84}/d_{16} , in which d_{16} (or d_{84})=sediment size for which 16 (or 84)% of the sample is finer; θ_1 and θ_2 =gradients of the main flume and the

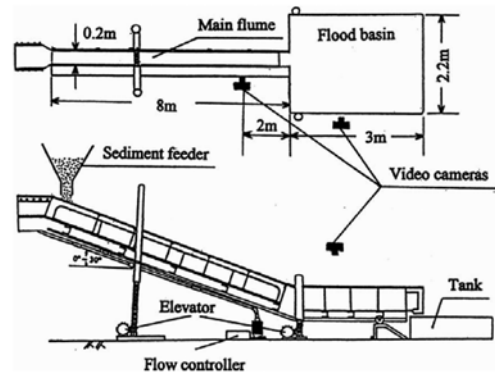


Fig. 1 - Schematic diagram of experimental setup in top view and side view

flood basin, respectively; Q_d =discharge of debris flow supplied at the upstream end of the main flume, and it is equal to the dry sediment discharge plus the mud flow or pure water discharge; C_d =the sediment volume concentration of debris flow formed in the main flume (computed as the ratio of dry sediment discharge and debris flow discharge); ρ =density of supplied pure water or mud fluid; L_m , B_m , and Z_0 denote, respectively, the measured maximum values of length, width, and thickness of debris-flow fans; and V is the measured volume in the flood basin for each experiment.

Notably, three kinds of sediments with uniform size ($C_u=1.0$) were used in experiments of Runs 1-30 ($d_{50}=1.6, 4.5,$ and 7.0 mm) to investigate the effects of sediment size, sediment volume concentrations, incline angles of the main flume, and the flood basin on the shape of a stony debris-flow fan. Sediments with granular mixture size ($C_u=2.5$ to 13) were used in the experiments conducted in Runs 31-57 to examine the influence of size distribution on the shape of a stony debris-flow fan. On the other hand, sediments with granular mixture size ($C_u=1.0$ to 13) and mud fluid ($\rho=1.0$ to 1.365) were used in the experiments of Runs 58-72 to study the effect on the shape of a mud debris-flow fan. The mud-fluid mixes lean clay and pure water with different volume concentrations (C_v) of 5, 13, and 22%. The median diameter of lean clay is about 0.016 mm. The densities (ρ) of the three mud fluids used in the experiments were 1.083, 1.216, and 1.365 g/cm³. Similar experiments were conducted by O'BRIEN & JULIEN (1986) and MAJOR & PIERSON (1992). Table 1 also lists three experiments (namely, Runs T1, T2, and T3) performed by TAKAHASHI (1980) to provide a comparison.

Run number	d_{50} (mm)	C_u	θ_1 (degree)	θ_2 (degree)	Q_d (cm ³ /s)	C_d (%)	ρ (g/cm ³)	l_c (cm)	B_m (cm)	Z_m (cm)	V (cm ³)
1	1.6	1.0	15	2	2.570	35.8	1.0	90	72	9.7	17.101
2	1.6	1.0	15	2	4.340	42.4	1.0	101	95	10.2	20.787
3	1.6	1.0	15	5	2.750	35.6	1.0	108	110	12.5	31.769
4	1.6	1.0	15	5	4.030	38.0	1.0	121	102	13.1	36.539
5	1.6	1.0	17	2	2.430	30.0	1.0	125	101	11.1	35.198
6	1.6	1.0	17	5	2.300	30.4	1.0	86	94	12.3	24.687
7	1.6	1.0	17	5	3.460	48.0	1.0	90	142	14.6	41.875
8	1.6	1.0	19	2	3.340	43.1	1.0	78	116	16.8	33.467
9	1.6	1.0	19	5	2.580	50.4	1.0	68	102	15.6	22.098
10	1.6	1.0	21	2	1.470	30.6	1.0	110	110	10.5	30.770
11	1.6	1.0	21	5	2.380	51.7	1.0	67	92	17.3	26.967
12	7.0	1.0	17	2	4.980	32.1	1.0	79	109	17.2	34.082
13	7.0	1.0	17	5	5.030	34.8	1.0	79	89	17.9	27.930
14	7.0	1.0	19	2	4.860	41.2	1.0	70	113	17.7	29.665
15	7.0	1.0	19	5	4.890	35.2	1.0	69	88	17.5	25.595
16	7.0	1.0	21	2	4.410	35.6	1.0	52	88	18.8	20.190
17	7.0	1.0	21	5	5.150	33.8	1.0	78	91	24.3	39.825
18	4.5	1.0	17	2	2.740	45.3	1.0	38	70	11.8	8.325
19	4.5	1.0	17	2	4.220	40.8	1.0	58	89	17.8	20.960
20	4.5	1.0	17	5	2.610	42.5	1.0	38	55	10.4	6.174
21	4.5	1.0	17	5	4.630	35.2	1.0	91	110	18.0	41.706
22	4.5	1.0	17	5	5.040	40.5	1.0	68	80	18.4	21.324
23	4.5	1.0	19	2	2.690	44.2	1.0	48	73	16.3	13.009
24	4.5	1.0	19	2	4.220	40.8	1.0	58	93	18.7	23.177
25	4.5	1.0	19	2	4.370	40.5	1.0	66	93	21.9	29.360
26	4.5	1.0	19	5	2.620	42.7	1.0	50	64	14.0	10.918
27	4.5	1.0	21	2	2.810	46.6	1.0	37	62	13.6	7.655
28	4.5	1.0	21	2	4.880	38.5	1.0	80	100	22.7	34.944
29	4.5	1.0	21	5	2.590	42.1	1.0	50	73	14.8	14.515
30	4.5	1.0	21	5	4.090	38.9	1.0	85	95	19.5	33.440
31	4.5	2.5	17	2	2.750	45.5	1.0	34	61	12.4	7.855
32	4.5	2.5	17	2	5.210	42.4	1.0	64	87	18.6	22.642
33	4.5	2.5	17	5	2.820	46.7	1.0	29	49	7.1	3.636
34	4.5	2.5	17	5	4.810	37.6	1.0	85	97	21.1	40.721
35	4.5	2.5	19	2	2.720	44.9	1.0	32	60	11.6	7.225
36	4.5	2.5	19	2	5.030	40.4	1.0	80	102	21.1	41.923
37	4.5	2.5	19	5	2.820	46.8	1.0	44	61	13.2	9.566
38	4.5	2.5	19	5	4.350	37.9	1.0	73	90	21.7	27.811
39	4.5	2.5	21	2	4.860	38.3	1.0	80	105	25.1	51.308
40	4.5	2.5	21	5	2.600	42.3	1.0	46	63	13.7	10.471
41	4.5	3.9	17	2	2.640	43.2	1.0	56	82	17.6	19.122
42	4.5	3.9	17	2	4.530	44.8	1.0	50	87	16.2	18.338
43	4.5	3.9	17	5	2.710	44.6	1.0	33	49	8.1	5.135
44	4.5	3.9	17	5	4.700	46.7	1.0	45	58	11.2	7.980
45	4.5	3.9	19	2	2.670	43.8	1.0	38	60	13.5	9.233
46	4.5	3.9	19	2	4.500	44.4	1.0	58	95	18.5	23.590
47	4.5	3.9	19	5	2.840	47.2	1.0	46	65	12.6	10.860
48	4.5	3.9	19	5	4.760	47.5	1.0	69	81	16.3	22.522
49	4.5	3.9	21	2	4.500	44.4	1.0	80	91	18.7	32.516
50	4.5	3.9	21	5	2.620	42.7	1.0	56	69	14.4	13.194
51	4.5	7.6	17	2	2.660	43.6	1.0	52	77	14.1	17.069
52	4.5	7.6	17	5	2.940	49.0	1.0	45	67	10.2	9.271
53	4.5	7.6	19	2	2.890	48.1	1.0	64	90	17.0	22.082
54	4.5	7.6	19	5	2.720	44.9	1.0	80	84	15.1	21.603
55	4.5	7.6	21	2	2.370	36.7	1.0	85	88	14.8	24.896
56	4.5	13.0	19	5	2.790	46.2	1.0	85	119	14.1	32.965
57	4.5	13.0	21	2	2.730	45.1	1.0	75	93	13.3	26.171
58	4.5	1.0	17	2	2.500	40.0	1.083	40	64	9.1	7.222
59	4.5	2.5	17	2	2.500	40.0	1.083	44	65	8.9	7.291
60	4.5	3.9	17	2	2.500	40.0	1.083	39	60	7.7	5.314
61	4.5	7.6	17	2	2.500	40.0	1.083	47	73	10.7	11.037
62	4.5	13.0	17	2	2.500	40.0	1.083	41	76	12.5	11.160
63	4.5	1.0	17	2	2.500	40.0	1.216	85	133	14.1	41.627
64	4.5	2.5	17	2	2.500	40.0	1.216	59	93	15.6	22.177
65	4.5	3.9	17	2	2.340	35.9	1.216	50	85	13.3	14.856
66	4.5	7.6	17	2	2.460	39.0	1.216	89	113	13.2	39.257
67	4.5	13.0	17	2	2.570	33.9	1.216	77	119	13.9	33.963
68	4.5	10	17	2	2.500	40.0	1.365	65	93	12.1	22.695
69	4.5	2.5	17	2	2.700	37.0	1.365	62	104	12.4	23.569
70	4.5	3.9	17	2	2.900	34.5	1.365	67	100	11.6	23.066
71	4.5	7.6	17	2	2.900	34.5	1.365	90	136	10.7	39.750
72	4.5	13.0	17	2	2.900	34.5	1.365	77	118	11.8	34.077
T1	5.05	1.0	17	2	1.200	50.0	1.0	81	79	9.7	13.279
T2	4.0	1.0	18	4	2.200	45.5	1.0	67	124	10.5	21.847
T3	4.0	1.0	18	4	2.200	36.4	1.0	75	142	13.0	32.996

Tab. 1 - Experimental conditions and results in the study

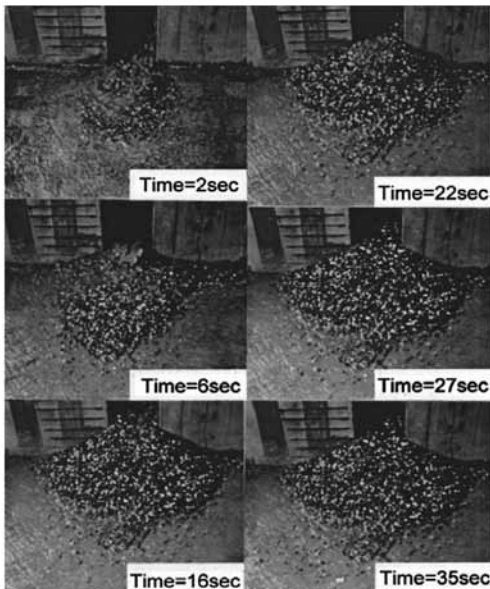


Fig. 2 - Temporal variations in shapes of Run 53

PROCESS OF FORMATION OF DEBRIS-FLOW FAN

The experimental results of Run 53 were adopted to describe the formation process of the debris-flow fan. The slopes of the main flume and flood basin for the case of Run 53 were set to 19° and 2° , respectively. Fig. 2 shows temporal variations in the shapes of Run 53. The time, indicated in the figures, was counted from the moment the forefront of the debris flow arrived at the mouth of the main flume (namely, the entrance of the flood basin). Fig. 3 shows the development of the maximum values of deposition length, width, and thickness of Run 53. In the earliest stage, when the debris flow debouched onto the flood basin, the path of the flow downstream from the main-flume outlet was straight, and the deposition length of the debris-flow fan quickly reached its maximum at 6 s. For a while, the flow drifted rightward and leftward, and its width and thickness build up with time. The deposition width of the debris-flow fan reached its maximum at 22 s, and the deposition is located on the connection between the main flume and flood basin. The deposition thickness of the debris-flow fan reached its maximum at 25 s and is located at the outlet of the main flume (namely, the apex of debris-flow fan). The period of fan development before 25 s is called the “developing stage.” During this stage, the maximum thickness and maximum width are not located at the outlet but at

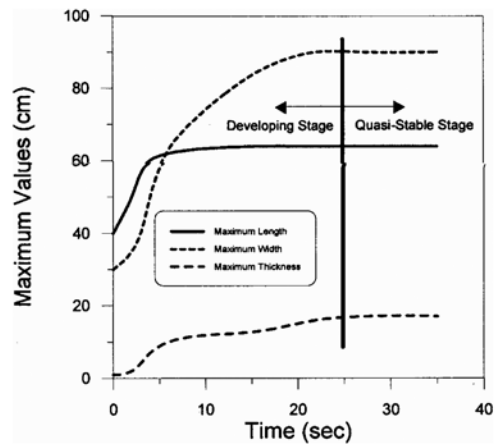


Fig. 3 - Developments of the maximum values of deposition length, width, and thickness of Run 53

some distance from it. Consequently, the debris-flow fan in the flood basin maintained its own shape and remained unchanged for a long period. This study refers to this stage of debris-flow fan development as the “quasi-stable stage.” During this stage, the deposition process proceeded upstream along the main flume, and the great part of the sediments was deposited on the main flume. Based on experimental observations, there are two important characteristics when the debris-flow fan reached the quasi-stable stage. First, there is a long-term subsidence of the debris-flow fan in the flood basin. Second, the maximum width and maximum thickness of the debris-flow fan will locate at the outlet of the main flume. On the other hand, if low-concentrated flow or water flow follows debris flow, the debris-flow fan will be eroded.

Fig. 4 displays the definitions of the debris-flow fan characteristic parameters for Run 10. Specifically, Fig. 4(a) shows the top view of the fringed shape of the debris-flow. At the intersection of the main flume and the flood basin, $X=0$. The positive value of X is downstream of the debris-flow fan. The central line of the debris-flow fan is indicated with $Y=0$, with positive values of Y denoting the left side of the debris-flow fan (viewed from upstream to downstream). Moreover, B is the width of the debris-flow fan at any section, and $B(X)$ decreases with increasing X . The maximum width of the debris-flow fan is B_m , and usually occurs at $X=0$ in the quasi-stable stage. Fig. 4(b) shows the longitudinal profile of the debris-flow fan. The length of the debris-flow fan is measured from the apex along the longitudinal axis. Usually, the maximum length is de-

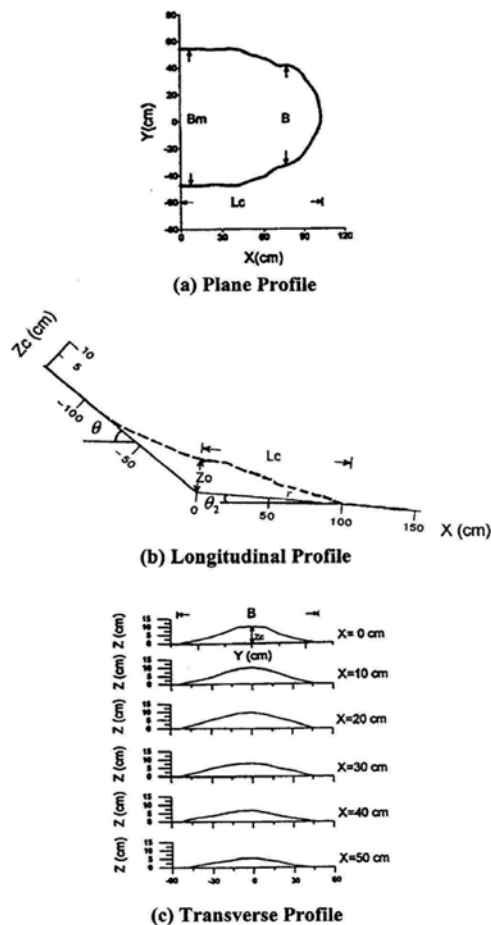


Fig. 4 - Definitions of debris-flow fan characteristic parameters

noted by L_c . The deposition thickness at $X=0$ and $Y=0$ is represented by Z_o , which is usually the maximum thickness of the debris-flow fan in the quasi-stable stage. Fig. 4(c) illustrates the transverse profile, where Z denotes the deposition thickness at any point, and Z_c represents the deposition thickness at the central point along the longitudinal axis. The variation of the debris-flow fan beyond the quasi-stable stage is not studied in this paper. This investigation focuses on the shape of the debris-flow fan in the quasi-stable stage.

DEBRIS-FLOW FAN CONFIGURATIONS
MORPHOLOGICAL SIMILARITY OF TRANSVERSE PROFILE

Thirty runs (Runs 1-30) of the present experimental results using uniform sediments ($C_u=1.0$), as well as three runs of Takahashi's (1980) (Runs T1-T3) were

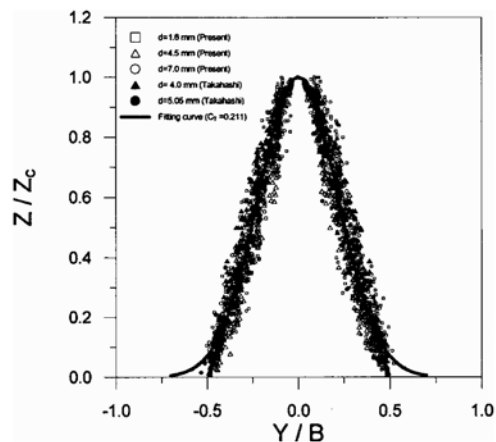


Fig. 5 - Relationship between Z/Z_c and Y/B via a Gaussian curve

adopted to analyze the transverse profile of stony debris-flow fan in the quasi-stable stage. About 280 transverse profiles were surveyed to analyze from Runs 1-30 and Runs T1-T3. The non-dimensional values of Z/Z_c against Y/B are illustrated in Fig. 5 and their relationship was approximated by a Gaussian curve with an empirical coefficient C_T , represented as Eq. 1.

$$\frac{Z}{Z_c} = \exp\left[-\frac{1}{2C_T^2}\left(\frac{Y}{B}\right)^2\right] \tag{1}$$

The best-fitting coefficient $C_T=0.211$, and the correlation coefficient is around 87%. In these experiments, the range of C_T is around 0.204-0.225, which varies insignificantly. A smaller C_T means a steeper Gaussian distribution. For stony debris-flow experiments (Runs 31-57) and mud debris-flow experiments (Runs 58-72), the non-dimensional transverse profile could also be approximated using a Gaussian curve, but the C_T increases with the uniformity coefficient C_u and the mud-fluid density ρ . For a natural stony debris-flow fan (with a very large C_u and $\rho=1.0$), the value of C_T is approximately 0.248.

MORPHOLOGICAL SIMILARITY OF LONGITUDINAL PROFILE

Thirty runs (Runs 1-30) of the present experimental results with uniform sediments ($C_u=1.0$) and three runs of Takahashi's (1980) (Runs T1-T3) were used to analyze the longitudinal profile of stony debris-flow fan in the quasi-stable stage. Fig. 6 plots the non-dimensional values of Z/Z_o against X/L_c , and their relationship were approximated by a half-Gaussian curve with an empirical coefficient C_L , represented as Eq. 2.

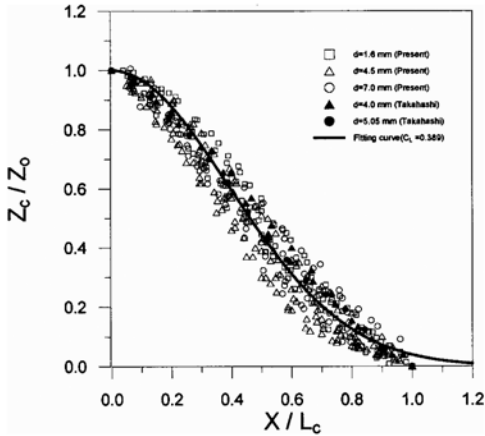


Fig. 6 - Relationship between Z_c/Z_o and X/L_c via a half-Gaussian curve

$$\frac{Z_c}{Z_o} = \exp\left[-\frac{1}{2C_L^2}\left(\frac{X}{L_c}\right)^2\right] \quad (2)$$

The best-fitting coefficient $C_L=0.389$, and the correlation coefficient is approximately 91%. In these experimental runs, the range of C_L is around 0.373~0.401. This variation is insignificant. For stony debris-flow experiments (Runs 31-57) and mud debris-flow experiments (Runs 58-72), the non-dimensional longitudinal profile were also approximated via a half-Gaussian curve. However, the results shows that C_L increases with the uniformity coefficient C_u and fluid density ρ . For a natural stony debris-flow fan (with a very large C_u and $\rho=1.0$), the value of C_L is approximately 0.416.

MORPHOLOGICAL SIMILARITY OF PLANE PROFILE

Let B denote the width of a stable debris-flow fan at any section X , while B_m represents the maximum width of that flow fan, which generally occurs at $X=0$; L_c =maximum deposition length. Fig. 7 illustrates the relative width B/B_m as a function of the relative coordinate X/L_c . The relationship between B/B_m and X/L_c of 75 runs (Runs 1-72 and Runs T1-T3) were approximated by a quarter circle curve, with a correlation coefficient of up to 98%. The circle function represented as Eq. 3.

$$\left(\frac{B}{B_m}\right)^2 + \left(\frac{X}{L_c}\right)^2 = 1 \quad (3)$$

THREE-DIMENSIONAL TOPOGRAPHY OF DEBRIS-FLOW FANS

The 3D topography of debris-flow fan was derived as Eq. 4, obtaining from Eq. 1, 2, and 3.

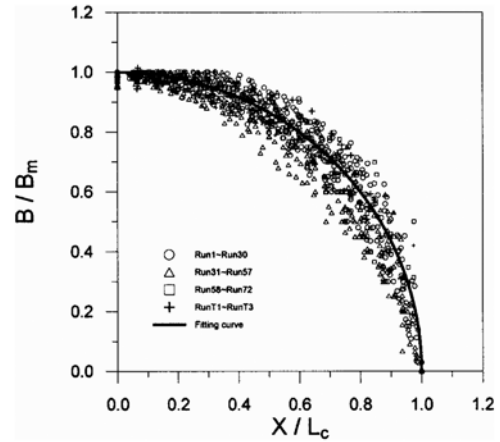


Fig. 7 - Relation between B/B_m and X/L_c via a quarter circle curve

$$Z = Z_o \exp\left[-\frac{X^2}{2C_L^2 L_c^2} - \frac{Y^2 L_c^2}{2C_T^2 B_m^2 (L_c^2 - X^2)}\right] \quad (4)$$

By the Eq. 4, the volume formula of debris-flow fan was derived from $Z = f(X, Y, L_c, B_m, Z_o)$, represented as Eq. 5

$$V = \alpha L_c B_m Z_o \quad (5)$$

Where α =function of the shape parameters C_T and C_L , represented as Eq. 6.

$$\alpha \approx 2C_T C_L \sqrt{\pi} \operatorname{erf}\left(\frac{1}{2\sqrt{2}C_T}\right) \left[\frac{\sqrt{\pi}}{2} \left(1 - \frac{3}{2}C_L^2\right) \operatorname{erf}\left(\frac{1}{\sqrt{2}C_L}\right) + \frac{C_L}{2\sqrt{2}}(1 + 3C_L^2)e^{-1/2C_L^2} \right] \quad (6)$$

The best Gaussian distribution coefficients, C_T and C_L , for each run were substituted into Eq. 6 to yield the values α . For 30 runs (Runs 1-30) of the present experimental results using uniform sediments ($C_u=1.0$) as well as three runs of TAKAHASHI'S (1980) (Runs T1-T3), $C_T=0.211$, $C_L=0.393$ and α is about 0.24 from Eq. 6. For a natural stony debris-flow fan (with a very large C_u and $\rho=1.0$), $C_T=0.248$, $C_L=0.416$, and α is approximately 0.275 from Eq. 6. By Eq. 5 $V=\alpha L_c B_m Z_o$, via an empirical coefficient α , the volume V of debris-flow fan is related to the maximum length L_c , width B_m , and thickness Z_o . Therefore, the 3D topography of a debris-flow fan is easily derived based on the parameters L_c , B_m , and Z_o using three morphologically similar formulas. Namely, after L_c , B_m , and Z_o is estimated, and the potential hazard zone of each debris-flow field is obtained.



Fig. 8 - Debris-flow fan located on Foncho Village in Central Taiwan

CASE STUDY

STUDY AREA

The debris flow fan located in Foncho Village, Nantou County, Taiwan were studied in this study. We derived the basic data of the stream. The watershed area (A) of the stream is about 3 ha; length (L) of the stream is about 3 km; mean slope (θ_1) of the main flume is about 28° ; mean slope (θ_2) of the flood basin is 8.7° .

Debris-flow disaster was common in this area. The most serious disaster had occurred during the period of Typhoon Herb in 1996. Fig. 8 shows the debris-flow fan which occurred after Typhoon Herb. In this event, the discharged volume of debris flow was up to 450000cm^3 . The characteristic of sediments of debris-flow fan was investigated. Where B_0 denotes the mean slope of upstream is about 12m; mean diameter (d_{50}) of the materials is about 3.5cm; uniformity coefficient (C_u) is about 67.5; internal friction angle (ϕ) is about 35° ; kinematic friction angle (ϕ_k) is about 29° ; density (ρ) is about 2.65g/cm^3 ; sediment volumetric concentration (C_s) is about 0.65. In addition, the quantity of fine materials (median diameters $< 0.1\text{mm}$) is under 10%. With the characteristics mentioned above, the debris flow in Foncho Village was treated as a stony debris flow.

In order to understand the relation between the debris-flow hazard zone and hydrology, various theories and empirical formulas were used to calculate the hydrological characteristics of debris flow during the period of Typhoon Herb.

1. The estimate of volumetric concentration (C_d) of debris flow;

According to the equilibrium concentration formula of debris flow derived by TAKAHASHI (1977), represented as Eq. 7. The volumetric concentration of debris flow has an upper limit, where the value C_d is about 0.9 times of C_s .

$$C_d = \frac{\rho \tan \theta_1}{(\sigma - \rho)(\tan \phi - \tan \theta_1)} \quad (7)$$

2. The estimate of flow discharge (Q_d) (cms) of debris flow;

The relation between Q_d and rainfall intensity (I) (mm/hr) is shown as Eq. 8. Where C represents the runoff coefficient (assume as 0.8). The rainfall intensity (I) is used with 25-year frequency ($I_{25} = 132.1\text{ mm/hr}$).

$$Q_d = \frac{C_s}{C_s - C_d} \frac{CIA}{360} \quad (8)$$

3. The estimate of mean velocity (u) (m/sec) of debris flow;

With the constitutive relation BAGNOLD (1954) derived to predict the mean velocity (u) of debris flow, the Equation is shown as Eq.9. Where α_i is friction coefficient ($=0.073$). g is acceleration of gravity.

$$u = \frac{2}{5d_{50}} \left\{ \frac{g \sin \theta_1}{\alpha_i \sin \phi_k} \left[C_d + (1 - C_d) \frac{\rho}{\sigma} \right] \right\}^{1/2} \left[\left(\frac{C_s}{C_d} \right)^{1/3} - 1 \right] h^{3/2} \quad (9)$$

4. The estimate of mean flow depth (h) (m) of debris flow;

According to the law of conservation of mass in fluid mechanics, Q_d is represented as Eq. 10. The mean flow depth (h) of debris flow was derived from Substituting Eq.8 and Eq. 9 into Eq. 10 which yields $Q_d = f(h)$

$$Q_d = B_0 hu \quad (10)$$

After this series of calculations, the hydrological characteristics of debris flow located in Foncho Village during the period of Typhoon Herb could be obtained respectively. The value of flow discharge (Q_d), mean velocity (u), mean flow depth (h) and volumetric concentration (C_d) is approximately 493.2cms, 18.1m/sec, 2.27m and 58.5%.

THE CALCULATION OF THREE-DIMENSIONAL TOPOGRAPHY OF DEBRIS-FLOW

By combining the volume formula of debris-flow fan derived from the experiments and hydrological data, the 3D topography of a debris-flow fan can be easily derived based on the parameters L_c , B_m , and Z_0 . For this purpose, various theory and empirical formulas were used to calculate the debris-flow hazard zone of Foncho Village in Nantou county.

1. The estimate of maximum length (L_c) of debris-flow fan.;

In order to obtain the maximum length (L_c) of debris-flow fan, a formula TAKAHASHI (1991) proposed was adopted. Based on conservation of mass and momentum balance, the Equation was revised as Eq. 11:

$$L_c = \frac{U^2}{G} \quad (11)$$

where:

$$U = u \cos(\theta_1 - \theta_2) \left\{ 1 + \frac{[(\sigma - \rho)C_d K_a + \rho] \cos \theta_1 gh}{2[(\sigma - \rho)C_d + \rho] u^2} \right\}$$

$$G = \frac{(\sigma - \rho)gC_d \cos \theta_2 \tan \phi_k}{(\sigma - \rho) C_d + \rho} - g \sin \theta_2$$

K_a means the coefficient of active earth pressure, in which $K_a = \tan^2(45^\circ - \phi/2)$.

2. The estimate of maximum deposition thickness (Z_0) of debris-flow fan;

From the Fig. 4(b), the relation between maximum deposition es (at the apex of fan), mean deposition slope along the longitudinal axis (r) and maximum length (L_c) is represented as Eq. 12. Namely, if the value of r and L_c could be obtained, the maximum deposition thickness (Z_0) could be estimated from Eq. 12.

$$Z_0 \approx \tan(\gamma - \theta_2) L_c \quad (12)$$

The deposition slope of debris-flow fan was derived from TAKAHASHI (1991). Eq. 13 represents the critical deposition slope of debris-flow fan, where the H_0 represents a flow depth above the deposition layer, d is diameter of sediment.

$$\tan \gamma = \frac{C_s(\sigma - \rho) \tan \phi}{C_s(\sigma - \rho) + \rho(1 + H_0/d)} \quad (13)$$

The values, H_0 and d were difficult to and field investigations. By a series of analyses, TSAI (1999) had found a close relation between mean deposition slope along the longitudinal axis (r), unit flow discharge (q), volumetric concentration (C_d) and sediment diameters (d_{50}). Consequently, the Eq.14 was derived from Eq. 13.

$$\tan \gamma = \frac{C_s(\sigma - \rho) \tan \phi}{C_s(\sigma - \rho) + \rho \left[1 + 4.5 \times 10^{-4} C_d^{-6} \left(\frac{q^2}{gd_{50}^3} \right)^{1/3} \right]} \quad (14)$$

3. The estimate of maximum width (B_m) of debris-flow fan;

If the maximum length (L_c), mean deposition slope (r), and the volume of debris fan could be obtained, the B_m is estimated by Eq. 15. Substituting Eq. 12 into Eq. 5 yields the Eq. 15:

$$B_m = \frac{V}{\alpha \tan(\gamma - \theta) L_c^2} \quad (15)$$

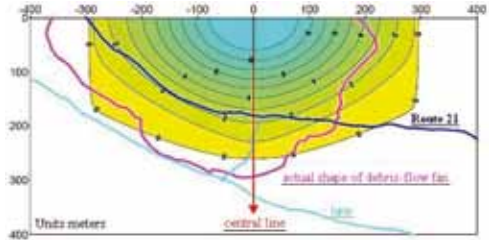


Fig. 9 - Topographies of the debris-flow fan in Foncho Village from experiments and field investigations

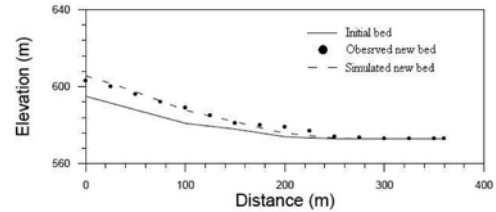


Fig. 10 - Changes of the bed of fan between experiments and field investigations

The maximum length, width and thickness of debris flow were estimated by substituting the hydrological characteristics into the formulas mention above. The maximum length (L_c) is about 262.4m, the mean deposition slope (r) is about 11.03° , maximum deposition thickness (Z_0) is about 10.6m, and the maximum width (B_m) is about 585.5m. By substituting the values of L_c , r , Z_0 and B_m into Eq.4, the 3D topography function of the debris-flow fan in Foncho Village was estimated by Eq. 16. Finally the hazard zone mapping of debris flow could be drawn as shown in Fig. 9.

$$Z = 10.6 \exp \left(-\frac{X^2}{23490} - 1.633 \frac{Y^2}{68850 - X^2} \right) \quad (16)$$

From the research results compared with the field investigations (Fig. 9), it shows that the proposed methods make a good hazard zone mapping of debris flow. In addition, the longitudinal profiles of central axis of debris-flow fan were both very similar in experiments and field investigations, as shown in Fig. 10. From the Fig. 10, we discovered that the observed new bed was higher than the simulated new bed only at the end of the debris-flow fan (at the distance of 200m). Consequently, the methods this research proposed can be applied to map the hazard zone of debris-flow fan.

CONCLUSIONS

This study presents labo ents and case study on the configurations of debris-flow fan. Seventy-five experimental tests (Runs 1-72, Runs T1-T3) show that

the profiles of debris-flow fan were approximated by Gaussian curves in both the longitudinal and transverse directions of the debris-flow path, while the shape of the fringe resembled a quarter circle curve. By combining the three non-dimensional curves, the volume V of debris-flow fan are related to the maximum length L_c , width B_m , and thickness Z_o by $V = \alpha L_c B_m Z_o$, via an empirical coefficient α . The 3D topography of a debris-flow fan are easily derived based on the parameters L_c , B_m , and Z_o using three morphologically similar formulas. Then, a debris-flow fan in Foncho

Village, Nantou County, Taiwan was investigated as an example. From the experimental results compared with the case study, it shows that the proposed methods make a good hazard zone mapping of debris flow. In conclusion, if L_c , B_m , and Z_o were estimated, the potential hazard zone of each debris-flow field could be divided into several different danger zones via the designed deposition thickness calculated from the 3D topography function. Such division is very useful for hazard zone mapping of debris flow.

REFERENCES

- ASHIDA K., TAKAHASHI T. & SAWADA T. (1980) - *Runoff process, sediment yield and transport in a mountain watershed*. Annuals of Disaster Prevention Research Institute, Kyoto University, **20**(B-2): 393-412, Kyoto, Japan.
- BAGNOLD R. A. (1954) - *Experiments on A Gravity-Free Dispersion of Large Solid Spheres in a Newtonian Fluid Under Shear*. Proceeding of Royal Society, Series A, **225**: 49-63, London.
- BATHURST J. C., BURTON A. & WARD T. J. (1997) - *Debris Flow Run-out and Landslide Sediment Delivery Model Tests*. Journal of Hydraulic Engineering, ASCE, **123**(5): 410-417.
- CANNON S. H. (1993) - *An Empirical Model for the Volume-Change Behaviour of Debris Flows*. Proceeding of 1993 Conference of Hydraulic Engineering, ASCE, 1768-1773, San Francisco, California, U.S.A.
- CETINA M. & KRZYK M. (2003) - *Two-dimensional mathematical modelling of debris flows with practical applications*. Proc. 2nd Int. Conf. on Water Resources Manage, 435-444.
- FRACCAROLLO L. & PAPA M. (2000) - *Numerical simulation of real debris-flow events*. Phys. Chem. Earth, Part B, **25**(9): 757-763.
- HOKE R. L. (1967) - *Processes on arid-region alluvial fans*. J. Geology, **75**: 405-460.
- ITOH T., MIYAMOTO K. & EGASHIRA S. (2003) - *Numerical simulation of debris flow over erodible bed*. Proc. 3rd Int. Conf. on Debris-Flow Hazards Mitigation, 457-468.
- IKEDA H. (1981) - *A Method of Designation for Area in Danger of Debris Flow: Erosion and Sediment Transport in Pacific Rim Steep lands*. Proceedings of Institute Associate Hydrology Science Symposium. IAHS, **132**: 576-568, Wallingford, U.K.
- LAIGLE D., HECTOR A. F., HÜBL J. & RICKENMANN D. (2003) - *Comparison of numerical simulation of muddy debris flow spreading to records of real events*. In: RICKENMANN D. & CHEN C.L. (eds) - *Debris-Flow Hazards Mitigation: Mechanics, Prediction, and Assessment*, Proceedings 3rd International DFHM Conference, Davos, Switzerland, 635-646, Millpress, Rotterdam.
- MAJOR J. J. & PIERSON T. C. (1992) - *Debris flow rheology: Experimental analysis of fine-grained slurries*. Water Resources Research, **28**(3): 841-857.
- O'BRIEN J. S. & JULIEN P. Y. (1986) - *Rheology of non-Newtonian fine sediment mixtures*. Proc. ASCE Specialty Conference on Aerodynamics, Fluid Mechanics and Hydraulics, ASCE, 989-996, New York
- OKUDA S. (1973) - *Field investigation of debris flow*. Annuals of Disaster Prevention Research Institute, Kyoto University, **16**(A): 53-69, Kyoto, Japan.
- OKUDA S., SUWA H., OKUNISHI K., NAKANO M. & YOKOYAMA K. (1977) - *Synthetic observation on debris flow: Part 3*. Annuals of Disaster Prevention Research Institute, Kyoto University, **20**(B-1): 237-263, Kyoto, Japan.
- OKUDA S. (1984) - *Features of Debris Deposits of Large Slope Failures Investigated from Historical Records*. Annuals of Disaster Prevention Research Institute, Kyoto University, **27**(B-1): 353-368, Kyoto, Japan.
- RICKENMANN D. & KOCH T. (1997) - *Comparison of debris flow modelling approaches*. Proc. 1st International Conference on Debris-Flow Hazards Mitigation, ASCE, 576-585, New York
- SHIEH C. L., JAN C. D. & TSAI Y. F. (1996) - *A numerical simulation of debris flow and its application*. Natural Hazards, **13**(1): 39-54.
- TAKAHASHI T. (1977) - *A Mechanism of Occurrence of Mud-Debris Flows and Their Characteristics in Motion*. Annuals of Disaster Prevention Research Institute, Kyoto University, **20**(B-2): 405-435, Kyoto, Japan..

- TAKAHASHI T. & YOSHIDA H. (1979) - *Study on the deposition of debris flow (1): Deposition due to abrupt change of bed slope*. Annuals of Disaster Prevention Research Institute, Kyoto University, **22**(B-2): 315-328, Kyoto, Japan.
- TAKAHASHI T. (1980) - *Study on the deposition of debris flow (2): Process of formation of debris-flow fan*. Annuals of Disaster Prevention Research Institute, Kyoto University, **23**(B-2): 443-456, Kyoto, Japan.
- TAKAHASHI T. (1991) - *Debris Flows*. International Association for Hydraulic Research, 221-223, Published by A. Balkema, Rotterdam, and Brookfield, Netherlands.
- TSAI Y.F. (1999) - *Study on the Configurations on Debris-Flow Fan*. PhD thesis, National Cheng Kung University, Taiwan.